Optical Engineering

RESEARCH PAPER

Optical system design of large-aperture space gravitational wave telescope

Miao Yu,[a] **Jiancong Li**,[a] **Hong'an Lin**,[a] **Yaozhang Huang**,[a] **Zhi Wang**,[b,c] **and Yanxiong Wu**[a,d,*]

[a]Foshan University of Science and Technology, School of Physics and Optoelectronic Engineering, Foshan, China

[b]Chinese Academy of Sciences, Changchun Institute of Optics, Precision Machinery and Physics, Jilin, China

[c]National University of Science and Technology, Hangzhou Institute for Advanced Study, School of Fundamental Physics and Mathematical Sciences, Hangzhou, China

[d]Jihua Laboratory, Foshan, China

ABSTRACT. In the Taiji Program, the space gravitational wave (GW) telescope is an important component of the space laser interferometer, which is used to receive and transmit laser signals, and has strict requirements in terms of light intensity signals and tilt-to-length (TTL) noise. Therefore, the telescope has a particular design; it should have a large aperture to meet the demand for light intensity signals, and the TTL coupling noise should be suppressed in the design process. Based on the primary aberration theory, the solution of the four-mirror off-axis initial structure is described. According to the interference model of flat-topped and Gaussian beams, the coupling coefficient of wavefront error and TTL noise at the exit pupil of the telescope are analytically calculated using the average phase signal. The optimization method and design flow are established, considering the special requirements of the space GW telescope. The results indicate that the diameter of the telescope entrance pupil is 400 mm, and the system magnification is 80×. The root mean square (RMS) value of wavefront errors is better than 0.00504 λ ($\lambda = 1064$ nm) within ± 8 μrad of the scientific field of view, and the coupling coefficient is not more than 1.7 pm/μrad within ± 600 μrad of jitter angle. The tolerance analysis of the design results shows that the RMS value and coupling coefficient meet the requirements of space GW detection. Therefore, the proposed design is a good candidate for the Taiji Program.

 [DOI: 10.1117/1.OE.62.6.065107]

Keywords: space gravitational wave detection; telescope; large aperture; Taiji Program

Paper 20230209G received Mar. 9, 2023; revised Jun. 10, 2023; accepted Jun. 12, 2023; published Jun. 23, 2023.

1 Introduction

Many gravitational wave (GW) sources in the universe are distributed in the frequency band 10^{-4} to 1 Hz; for example, double dense star systems and super- and medium-mass ratio double black hole rotation systems, which contain information on the early structure and evolution of the universe.[1]

To eliminate the limitation of the earth's curvature and the influence of gravitational gradient noise in the acquisition of the GW information in the frequency band 10^{-4} to 1 Hz, the space GW detection plan was proposed. This plan includes the laser interferometer space antenna (LISA), the Taiji project, and the Tianqin project.[2–5] All three comprise three spacecrafts each and are

*Address all correspondence to Yanxiong Wu, wuyanxiong@fosu.edu.cn

0091-3286/2023/$28.00

equilateral triangular space laser interferometric observatories with an interference arm length in the range of millions of kilometers. The telescope is a subsystem of the space laser interferometer, which is used to receive and transmit laser signals between two satellites separated by a distance of up to three million kilometers, measuring the optical path change between the local optical platform and that of the remote spacecraft; its optical path stability should satisfy the requirement of $1\ \mathrm{pm}/\sqrt{\mathrm{Hz}}$.[1,6,7]

As the spacecraft is easily disturbed by non-conservative forces in space, the beam received by the telescope is jittered. The wavefront error at the exit pupil of the system is coupled with tilt-to-length (TTL) noise, which is the main source of noise in the detection system after shot noise. According to existing literature, the LISA path finder (LPF) and average phase (AP) signals are two analytical methods used for calculating the coupling of wavefront error and TTL noise.[8] Compared to the LPF signal, the AP signal can reduce the coupling of TTL noise and wavefront error to a greater extent, thereby reducing the requirement for the wavefront error. In practical situations, several factors such as the imaging system, diaphragm position, and wave aberration at the exit pupil of the telescope affect TTL coupling noise. Although, it is difficult to quantitatively analyze the contribution of a single factor to TTL coupling noise, the noise source can be suppressed. Thus far,[8–13] Zhao presented a comprehensive theoretical analysis of the influence of telescope aberration on TTL coupling noise, proposed that the coupling coefficient should be suppressed at $\pm 25\ \mathrm{pm}/\mu\mathrm{rad}$, analyzed the contribution of TTL coupling noise of the prototype of the Taiji project telescope principle, and determined whether the final optical path stability has exceeded $3\ \mathrm{pm}/\sqrt{\mathrm{Hz}}$.[14]

Based on the current disclosed research related to GW telescopes,[11,15–18] Livas and Fan designed an off-axis four-mirror telescope with a magnification of 40× and an entrance pupil diameter of 200 and 220 mm, respectively. The LISA Consortium proposed a design index of 300 mm telescope. Chwalla developed a 350 mm telescope simulator to measure the TTL coupling noise. According to the Taiji project plan issued by the Chinese Academy of Sciences and the yellow book on the LISA plan issued by the European Space Agency and National Aeronautics and Space Administration (NASA),[3,7] the aperture of the space GW telescope, magnification, and scientific field of view were 400 mm, 80×, and $\pm 8\ \mu\mathrm{rad}$, respectively. This is because the laser intensity between the two satellites becomes very weak after three million kilometers of transmission, significantly impacting the phase extraction of the interference signal. Therefore, a telescope with a larger aperture is required to receive the laser signal to satisfy the light intensity requirements for the measuring beam. The aperture of the telescope has thus increased from 200 to 400 mm, making it more difficult to control the primary spherical and coma aberrations of the system. Moreover, strict requirements for wavefront error and optical path stability should be satisfied, thereby making the design process more challenging.

In a previous work, we studied the principal prototype of the 200-mm-aperture space GW telescope.[14–18] In the current Taiji project mission, we have developed a 400-mm-aperture telescope to detect GWs in the frequency band 10^{-4} to 1 Hz. In this study, according to the Taiji telescope requirements and based on the primary aberration theory, we have established a coaxial four-mirror initial structure with an aperture of 400 mm, which eliminates the central occlusion through the off-axis aperture. As the coupling of telescope wavefront error and TTL noise significantly affects the stability of interferometric precision measurement, we analyze the coupling coefficient between them through AP signals and establish an optimization strategy and design process for the control requirements of the Taiji telescope in terms of wavefront error and coupling coefficient. Finally, we examine the tolerance of the telescope to ensure that its wavefront error and coupling coefficient can meet the manufacturing requirements within the reasonable tolerance range. Subsequently, the final design results are obtained.

2 Initial Structural Design of the Telescope

2.1 Design Specifications

In the Taiji project, the telescope plays an important role in the precision measurement of space laser interference. Unlike traditional imaging telescopes, it is mainly used for receiving and transmitting laser signals. Therefore, it not only needs excellent wavefront quality to maximize the energy transmission efficiency but also must meet the noise control requirements of GW

Table 1 Optical system index of the space GW telescope.

Style name	Brief description
Aperture (mm)	400
Wavelength (nm)	1064
Scientific field of view (μrad)	±8
Magnification	80×
System wave aberration	≤0.05 λ @ 1064 nm
Coupling coefficient (pm · μrad^{-1})	≤25

measurement. The key parameters and indicators of the telescope are listed in Table 1. The diameter of the entrance pupil of the telescope was set to 400 mm to improve the light intensity signal of the space laser interferometer.[3,7] Because the transmission efficiency of laser beam energy is proportional to the square of Strehl ratio, the Strehl ratio to meet the diffraction limit is required to be 0.8, and the corresponding wavefront error control requirement is 0.05 λ ($\lambda = 1064$ nm). Therefore, the wavefront error of Taiji telescope should be <0.05 λ to achieve higher energy transmission efficiency.[1] More importantly, to analyze the complete GW signal, the coupling coefficient between wavefront error and TTL noise should be suppressed within ± 25 pm/μrad.[8–13]

2.2 Initial Structural Design

Spherical aberration, coma aberration, astigmatism, field curvature, and distortion are common aberrations in reflective optical systems. The wave aberration of the optical system can be expressed using Seidel coefficients as follows:

$$W(\rho,\theta,y) = \frac{1}{8}S_I\rho^4 + \frac{1}{2}S_{\mathrm{II}}\rho^3 y\ \cos\,\theta + \frac{1}{2}S_{\mathrm{III}}\rho^2 y^2 \cos^2\theta + \frac{1}{4}(S_{\mathrm{III}} + S_{\mathrm{IV}})\rho^2 y^2 + \frac{1}{2}S_V \rho y^3\ \cos\,\theta. \tag{1}$$

Here, (ρ,θ) are the polar coordinates and y is the field factor. S_{I}, S_{II}, S_{III}, S_{IV}, and S_{V} are the primary Seidel aberration coefficients, corresponding to spherical aberration, coma aberration, astigmatism, field curvature, and distortion, respectively. The spherical aberration is proportional to the fourth power of the aperture ρ of the telescope, the coma aberration is proportional to the cubic and field factor y of aperture ρ, and the astigmatism and field curvature are proportional to the quadratic and field factor y of aperture ρ. When the scientific field of view is maintained constant and the aperture of the system is increased from 200 to 400 mm, the aperture increases twice, and the primary spherical and coma aberrations worsen by 16 and 8 times, respectively.

The telescope of the Taiji project is designed with an off-axis aperture such that the backward stray light of the coaxial four-mirror telescope is directly transmitted to the detector, thereby having a more significant impact on the interference signal.[19,20] In addition, the system has an off-axis four-mirror unfocused optical path structure of the middle image plane, which is divided into objective lens and eyepiece. The primary mirror (PM) and secondary mirror (SM) constitute the objective lens of the telescopic system, whereas the tertiary mirror (TM) and quaternary mirror (QM) constitute the eyepiece. The first image plane is located between the SM and TM. Therefore, we first adopted the initial structure of the classic Cassegrain telescope, as shown in Fig. 1, and then design it with an off-axis aperture. In Fig. 1, PM, SM, TM, and QM denote the four mirrors; d_i denotes the distance between the mirrors; R_i is the radius of curvature of the mirrors; l_i and l_i' are the object and image distances of the corresponding mirrors, respectively.

After deduction, the initial structural parameters of the telescope optical system can be expressed as

$$\begin{cases} R_2 = \frac{R_1\alpha_1\beta_1}{1+\beta_1} \\ R_3 = \frac{R_1\alpha_1\alpha_2\beta_1\beta_2}{1+\beta_2} \\ R_4 = R_1\alpha_1\alpha_2\alpha_3\beta_1\beta_2 \end{cases}, \tag{2}$$

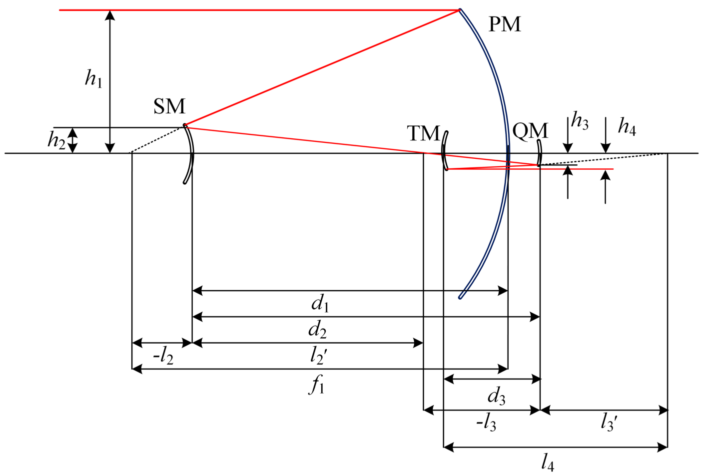

Fig. 1 Initial structure of the optical system.

$$\begin{cases} d_1 = \frac{R_1(1-\alpha_1)}{2} \\ d_2 = \frac{R_1\alpha_1\beta_1(1-\alpha_2)}{2} \\ d_3 = \frac{R_1\alpha_1\alpha_2\beta_1\beta_2(1-\alpha_3)}{2} \end{cases}, \tag{3}$$

where α_1 is the occlusion ratio of SM to PM, α_2 is the occlusion ratio of TM to SM, and α_3 is the occlusion ratio of QM to TM. β_1 is the magnification of SM, and β_2 is the magnification of TM. These can be expressed as

$$\begin{cases} \alpha_1 = \frac{l_2}{f_1} \approx \frac{h_2}{h_1} \\ \alpha_2 = \frac{l_3}{l_2'} \approx \frac{h_3}{h_2} \\ \alpha_3 = \frac{l_4}{l_3'} \approx \frac{h_4}{h_3} \end{cases}, \tag{4}$$

$$\begin{cases} \beta_1 = \frac{l_2'}{l_2} = \frac{u_2}{u_2'} \\ \beta_2 = \frac{l_3'}{l_3} \approx \frac{u_3}{u_3'} \end{cases}. \tag{5}$$

According to Eqs. (2)–(5), the structural parameters d_i and R_i of the optical system are determined using α_i and β_i. The aperture of the Taiji telescope is in the PM, and for the defocused system, the object distance of the PM is $l_1 = \infty$, and the object square aperture angle is $u_1 = 0$. The effective aperture of the SM is $D_1 \approx 40$ mm; therefore, the off-axis of the PM is set to 250 mm, and its size is $D_1 = 900$ mm. The QM image distance is $l_4 = \infty$, and the image square aperture angle is $u_4 = 0$. The power of the system is mainly borne by the PM and SM. Considering the limitation of the system length and PM sensitivity, the F number of the PM is set to approximately 1.8; therefore, the radius of curvature of the PM is set to $R_1 = 1500$ mm. After solution optimization and determination, the initial structural parameters of the telescope obtained are listed in Table 2.

Table 2 Structural parameters of the optical system.

Structural parameters	Value
α_1	0.07143
α_2	−0.09714
α_3	1.80147
β_1	−14
β_2	−1.25104

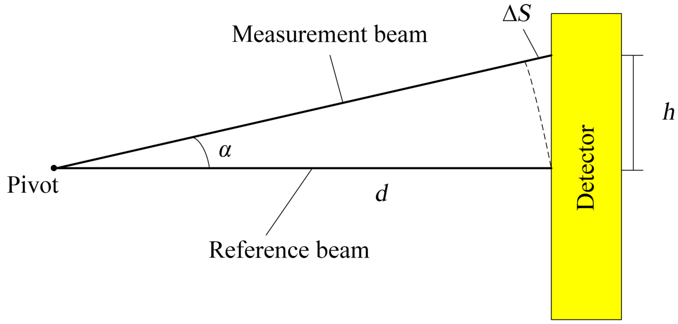

Fig. 2 Schematic diagram of TTL noise.

3 Analytical Calculations of TTL Coupling Noise

In the space environment, the spacecraft attitude inevitably jitters due to non-conservative forces, such as solar wind and solar radiation. This jitter can cause the transmission direction of the beam to shake when the telescope receives or emits the beam, resulting in the path length signal of the beam being measured for a longer distance. The noise formed by the coupling between beam jitter and path length is collectively referred to as TTL noise,[21] as shown in Fig. 2. Among them, d is the optical path from the reference beam to the center of the detector, h is the height of the measuring beam on the detector, and α measures the inclination angle of the beam. When the reference beam hits the center of the detector vertically, the measuring beam strikes the detector at an inclined angle. Therefore, the measurement beam takes an extra ΔS path relative to the reference beam, and this additional path due to tilt is coupled into the final measurement path signal.

In this section, we use AP signal analysis to calculate the coupling coefficient of the wavefront error and jitter optical path noise at the exit pupil of the telescope to judge whether the design results satisfy the requirements of the indicators. The space laser interferometer receives the measurement beam sent by the remote spacecraft through the telescope, and after propagation, it interferes with the local Gaussian beam on the quadrant photodiode (QPD). The corresponding phase information is calculated by extracting the complex amplitude of the interference signal in each quadrant. Finally, the final phase information of the entire interferometry system is obtained by considering the AP of the four quadrants. As shown in Fig. 3, to facilitate the analytical calculation, we assume that the centers of the flat top beam E_{flat} and Gaussian beam E_{Gauss} are coincident with the center of the QPD. Considering the phase calculation of the first quadrant as an example, the complex amplitude A and phase ϕ_A can be expressed as follows:

$$A = \int_{S_A} E_{\text{flat}} E^{*}_{\text{Gauss}} \mathrm{d}r^2 = \int_0^1 \rho e^{-\rho^2/\omega_r^2} \left(\int_0^{\frac{\pi}{2}} e^{ikW(\rho,\theta)} \mathrm{d}\theta \right) \mathrm{d}\rho, \tag{6}$$

$$\varphi_A = \arg(A), \tag{7}$$

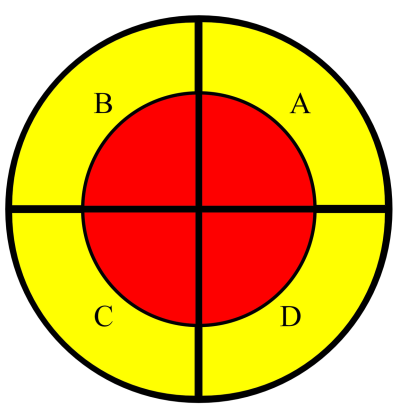

Fig. 3 Schematic of the interference beam on the four-quadrant detector.

where (ρ, θ) are the polar coordinates on the detector, $\omega(z)$ is the spot size on the detector, and $W(\rho, \theta)$ is the total wavefront error of the system.

As Zernike polynomials are orthogonal in the circular domain and correspond to Seidel aberrations, they are often used as the orthogonal basis for wavefront reconstruction. Therefore, the total wavefront error of the system is represented by the first 25 Fringe Zernike polynomials as follows:

$$W(\rho, \theta) = \sum_{i=1}^{25} a_i Z_i(\rho, \theta), \tag{8}$$

$$Z_i(\rho, \theta) = \begin{cases} \sqrt{2(n+1)} R_n^m(\rho) \cos(m\theta) & i \text{ is even and } m \neq 0 \\ \sqrt{2(n+1)} R_n^m(\rho) \sin(m\theta) & i \text{ is odd and } m \neq 0 \\ \sqrt{(n+1)} R_n^m & m = 0 \end{cases}, \tag{9}$$

$$R_n^m(\rho) = \sum_{s=0}^{n-m} \frac{(-1)^s (n-s)!}{s! \left(\frac{n+m-s}{2}\right)! \left(\frac{n-m-s}{2}\right)!}, \tag{10}$$

where $R_n^m(\rho)$ is the radial polynomial; s, n, and m are integers where $n - m \geq 0$; and $\rho = r/R$ is the normalized radial coordinate. To simplify the following analytical calculation, the cosine and sine terms of the same aberration are combined

$$a_i Z_i \cos(\theta) + a_{i+1} Z_{i+1} \sin(\theta) = A_j^{\text{aber}} Z_j \cos(\theta - \theta_{Ti}), \tag{11}$$

$$A_j^{\text{aber}} = \sqrt{a_i^2 + a_{i+1}^2}, \quad \theta_{\text{aber}} = \tan^{-1}\left(\frac{a_{i+1}}{a_i}\right), \tag{12}$$

where A_j^{aber} and θ_{aber} are the amplitude and direction angle of the combined aberration, respectively. The corresponding expressions and aberrations are given in Table 3, where A_1^{TI} can be replaced by the pointing jittery angle α. Therefore, Eq. (8) can be further expressed as

$$W(\rho, \theta) = 2\alpha\rho \cos(\theta - \theta_{TI}) + \sum_{j=2}^{14} A_j^{\text{aber}} Z_j(\rho, \theta). \tag{13}$$

Table 3 Aberrations after merging the first 25 Fringe Zernike polynomials.

A_j^{aber}	$Z_j(\rho, \theta)$	Aberration name
A_1^{TI}	$2\rho \cos(\theta - \theta_{\text{TI}})$	Tilt (TI)
A_2^{DE}	$\sqrt{3}(2\rho^2 - 1)$	Defocus (DE)
A_3^{PA}	$\sqrt{6}\rho^2 \cos(2\theta - \theta_{\text{PA}})$	Primary astigmatism (PA)
A_4^{PC}	$\sqrt{8}(3\rho^3 - 2\rho)\cos(\theta - \theta_{\text{PC}})$	Primary coma (PC)
A_5^{PS}	$\sqrt{5}(6\rho^4 - 6\rho^2 + 1)$	Primary spherical (PS)
A_6^{PTR}	$\sqrt{8}\rho^3 \cos(3\theta - \theta_{\text{PTR}})$	Primary trefoil (PTR)
A_7^{SA}	$\sqrt{10}(4\rho^4 - 3\rho^2)\cos(2\theta - \theta_{\text{SA}})$	Secondary astigmatism (SA)
A_8^{SC}	$\sqrt{12}(10\rho^5 - 12\rho^3 + 3\rho)\cos(\theta - \theta_{\text{SC}})$	Secondary coma (SC)
A_9^{SS}	$\sqrt{7}(20\rho^6 - 30\rho^4 + 12\rho^2 - 1)$	Secondary spherical (SS)
A_{10}^{PTE}	$\sqrt{10}\rho^4 \cos(4\theta - \theta_{\text{PTE}})$	Primary tetrafoil (PTE)
A_{11}^{STR}	$\sqrt{12}(5\rho^5 - 4\rho^3)\cos(3\theta - \theta_{\text{STR}})$	Secondary trefoil (STR)
A_{12}^{TA}	$\sqrt{14}(15\rho^6 - 20\rho^4 + 6\rho^2)\cos(2\theta - \theta_{\text{TA}})$	Tertiary astigmatism (TA)
A_{13}^{TC}	$4(35\rho^7 - 60\rho^5 + 30\rho^3 - 4\rho)\cos(\theta$	Tertiary coma (TC)
A_{14}^{TS}	$3(70\rho^8 - 140\rho^6 + 90\rho^4 - 20\rho^2 + 1)$	Tertiary spherical (TS)

The phase calculation method of the other three quadrants is the same as that of the first quadrant. Therefore, the AP signal obtained in the QPD analytic calculation can be expressed as

$$\varphi_{\mathrm{AP}} = \frac{\arg(A) + \arg(B) + \arg(C) + \arg(D)}{4} = \frac{\varphi_A + \varphi_B + \varphi_C + \varphi_D}{4}. \tag{14}$$

In the analysis, the items unrelated to α and higher than the second order are ignored. Therefore, the optical path error (OPE) of the system is the ratio (φ_{AP}/k) of φ_{AP} and wavenumber k, which is analytically obtained using Eq. (14)

$$\mathrm{OPE} = F_1 \times \alpha + F_2 \times \alpha^2, \tag{15}$$

$$F_1 = v_1 \times M_1 \times v_2^T, \tag{16}$$

$$F_1 = v_1 \times M_1 \times v_2^T, \tag{17}$$

$$v_1 = [A_4^{\mathrm{PC}}, A_8^{\mathrm{SC}}, A_{13}^{\mathrm{TC}}, A_6^{\mathrm{PTR}}, A_{11}^{\mathrm{STR}}], \tag{18}$$

$$v_2 = [A_2^{\mathrm{DE}}, A_5^{\mathrm{PS}}, A_9^{\mathrm{SS}}, A_{14}^{\mathrm{TS}}, A_3^{\mathrm{PA}}, A_7^{\mathrm{SA}}, A_{12}^{\mathrm{TA}}, A_{10}^{\mathrm{PTE}}], \tag{19}$$

where M_1 and M_2 are coefficient matrices, in which the specific expression is shown in the Mathematica code (Code 1 in the supplementary material[22]). The coupling coefficient δ between TTL noise and wavefront error is calculated by deriving α using Eq. (15) as

$$\delta = F_1 + 2F_2 \times \alpha, \tag{20}$$

4 Design and Optimization

The performance of the Taiji telescope is different from that of traditional imaging telescope systems. Therefore, it is necessary to analyze the wavefront error W and coupling coefficient δ simultaneously. In addition, within the scientific field of view, the wavefront error and coupling coefficient should not be significantly affected by the change of the field of view.

The current optical design software only provides the default evaluation function to control the root mean square (RMS) value of the wavefront error and cannot directly optimize the coupling coefficient δ. Therefore, it is necessary to optimize both the wavefront error W and coupling coefficient δ via the self-compiled optimization function. As the ZEMAX optical design software can extract Fringe Zernike polynomial coefficients, which can enable the determination of optimization functions to optimize coupling coefficients, ZEMAX is used to optimize the design. First, we extracted the coefficients of 25 Fringe Zernike polynomials using ZERN operands. According to Eqs. (11) and (12), we combined similar terms of the polynomials into 14 terms through the relevant operands and obtained the coefficients of these terms. In addition, as the Fringe Zernike polynomial coefficients proposed in ZEMAX contain constant terms, it is necessary to divide the constant term to obtain the accurate amplitude A_j^{aber}. Subsequently, we calculated the specific values of the coefficient matrices, M_1 and M_2, with a program using the software Mathematica. We then calculated the coupling coefficient using Eq. (20), and suppressed it to ± 25 pm$/\mu$rad. Simultaneously, we can use the amplitude A_j^{aber} to calculate and control the wavefront error of the system using Eq. (5). Therefore, we could control the wavefront error and coupling coefficient simultaneously by applying the aforementioned methods.[23] According to the special design requirements of the Taiji telescope, we have established the design flowchart for optimization, as shown in Fig. 4.

The initial structure parameters of the telescope, calculated in Sec. 2, were combined with the dual control optimization function of wavefront error and coupling coefficient established in this section, and the progressive optimization strategy was adopted to carry out the optimization design. As the aperture of the PM is large, considering the influence of manufacturing errors, it is set as a paraboloid, that is, the conic coefficient is set to -1. The SM is set to be an even degree aspherical surface, and the number of high-order items gradually increases during the optimization process, with the highest item being the 10th. The TM and QM are set as spheres,

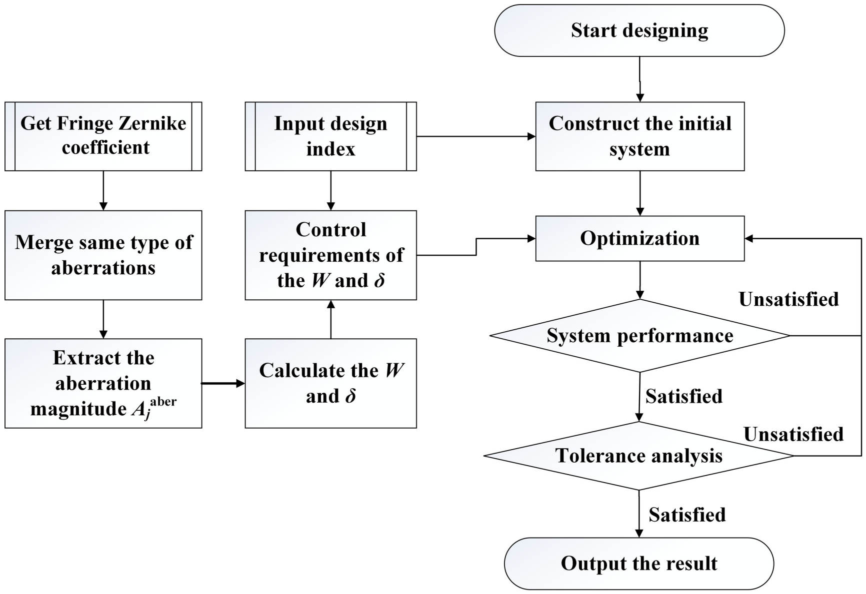

Fig. 4 Flowchart of the design and optimization of the Taiji telescope.

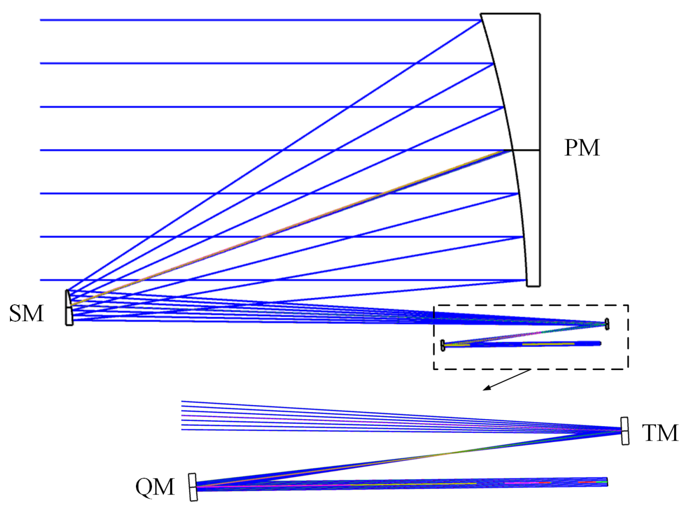

Fig. 5 Optimized telescope system structure.

and they are tilted at a certain angle along the x-direction to ensure that the telescope has a real exit pupil, which is convenient for the overall layout of the interferometer. The structure of the finally designed optical system is shown in Fig. 5, the design parameters of each mirror of the telescope are shown in Table 4, and the high-order coefficient of the SM is shown in Table 5.

Table 4 Optimized design parameters of the telescope optical system.

Mirror	Radius (mm)	Distance (mm)	Conic
PM	−1598.638	−750	−1
SM	−105.482	820	−1.28214
TM	−987.908	−100	—
QM	352.881	150	—

Table 5 Higher-order coefficients of even-order aspheric surfaces of the secondary mirror.

Number of items	4th	6th	8th	10th
Coefficient	3.589×10^{-13}	-4.123×10^{-15}	-4.927×10^{-16}	2.358×10^{-22}

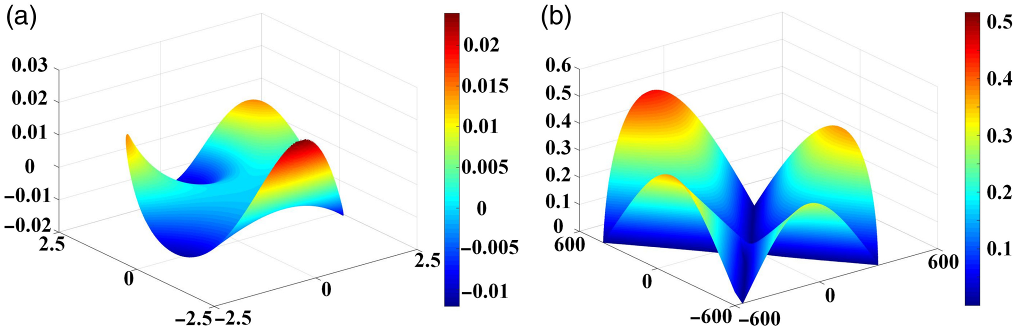

Fig. 6 (a) Wavefront at the exit pupil of the telescope after optimization. (b) TTL coupled noise calculation results.

5 Design Results and Tolerance Analysis

5.1 Analysis of Design Results

We analyzed the wavefront error and coupling coefficient according to the design results presented in Sec. 4. Figure 6(a) shows the wavefront error at the exit pupil on the telescope axis. The RMS value of the wavefront error is $0.00504\,\lambda$, and the peak-valley (P-V) is $0.03616\,\lambda$. The RMS value and P-V of each field point are listed in Table 6. The maximum error of the RMS value in the full field of view is $0.00001\,\lambda$, and the P-V error is $0.0015\,\lambda$; thus, they are consistent within the scientific field of view. In this study, we analyzed the wavefront at the axial field of view. The magnitude (Mag) and orientation (Ori) fitted by the Fringe Zernike polynomials are listed in Table 7. The wavefront aberration of the system is mainly primary trefoil (PTR) aberration. The coupling coefficient calculated according to Eq. (20) is shown in Fig. 5(b), and the maximum value of the coupling coefficient does not exceed 1.7 pm/μrad within ± 600 μrad, which is lower than the index requirement of 25 pm/μrad. Therefore, the detection requirements of the Taiji project were satisfied.

5.2 Tolerance Analysis

To further determine whether the design results can satisfy the requirements of the wavefront error and coupling coefficient change in manufacturing links, such as processing and assembly,

Table 6 Wavefront error at the exit pupil of each field of view.

Field (μrad)	RMS ($\lambda = 1064$ nm)	P-V ($\lambda = 1064$ nm)	δ (pm/μrad)
(0, 0)	$0.00504\,\lambda$	$0.03616\,\lambda$	1.6857
(5.6, 0)	$0.00504\,\lambda$	$0.03606\,\lambda$	1.6555
(8.0, 0)	$0.00504\,\lambda$	$0.03606\,\lambda$	1.6432
(0, 5.6)	$0.00503\,\lambda$	$0.03602\,\lambda$	1.6992
(0, 8.0)	$0.00503\,\lambda$	$0.03601\,\lambda$	1.7102
(5.6, 5.6)	$0.00503\,\lambda$	$0.03602\,\lambda$	1.6628
(8.0, 8.0)	$0.00503\,\lambda$	$0.03601\,\lambda$	1.6556
(0, 0)	$0.00504\,\lambda$	$0.03616\,\lambda$	1.6857

Table 7 Amplitude and orientation of the wavefront at the exit pupil of a telescope based on Zernike polynomials.

Mag/Ori	A_2^{DE}	A_3^{PA}/θ_{PA}	A_4^{PC}/θ_{PC}	A_5^{PS}	A_6^{PTR}/θ_{PTR}	A_7^{SA}/θ_{SA}	A_8^{SC}/θ_{SC}
nm/rad	0.4964	0.0508/0	0.1610/1.57	0.9764	4.7956/1.57	1.5834/0	0.2589/3.14
Mag/Ori	A_9^{SS}	$A_{10}^{PTE}/\theta_{PTE}$	$A_{11}^{STR}/\theta_{STR}$	A_{12}^{TA}/θ_{TA}	A_{13}^{TC}/θ_{TC}	A_{14}^{TS}	—
nm/rad	0.2337	0.2337	1.0437/0	0.1235/3.14	0.3239/0	0.2405/3.14	—

Table 8 Tolerance distribution results with coupling coefficient as the control requirement.

Type	Manufacturing error	PM	SM	TM	QM
Radius	ΔR/mm	0.3	0.1	1.4	1.4
Conic	Δk	0.0001	0.0004	—	—
Surface	RMS(λ)	1/60	1/60	1/100	1/100
Decenter	$\Delta d_x/\mu$m	—	10	20	20
	$\Delta d_y/\mu$m	—	10	20	20
Distance between mirrors	$\Delta d_z/\mu$m	—	10	20	20
Tilt	$\Delta T_x/''$	—	20	40	40
	$\Delta T_y/''$	—	20	40	40
	$\Delta T_z/''$	—	20	40	40

tolerance analysis is required for the telescope. In the analysis of the machining tolerance of the telescope optical system, the radius of the mirror, surface error, and conic coefficients of the PM and SM are mainly considered. When the PM is used as the installation and adjustment benchmark, the SM, TM, and QM each have six degrees of freedom, which are the rigid body displacement and tilt in the x-, y-, and z-direction. The specific tolerance distribution of processing, assembly, and adjustment considered in this study is listed in Table 8. To judge whether the tolerance analysis results satisfied the Taiji mission requirements, the wavefront error and Fringe Zernike polynomial amplitude of 500 tolerance analysis files were extracted, and the change of coupling coefficient was calculated and analyzed using Eq. (20). The analysis result corresponding to the tolerance file is shown in Fig. 7, and the wavefront error with 99.8% cumulative probability is $<0.05\,\lambda$. The cumulative probability of 99.4% of the coupling coefficient is within ± 25 pm/μrad, and the average value is 9.8 pm/μrad. Therefore, the wavefront error and coupling coefficient satisfied the requirements under typical tolerance conditions, and therefore, the design results were realizable.

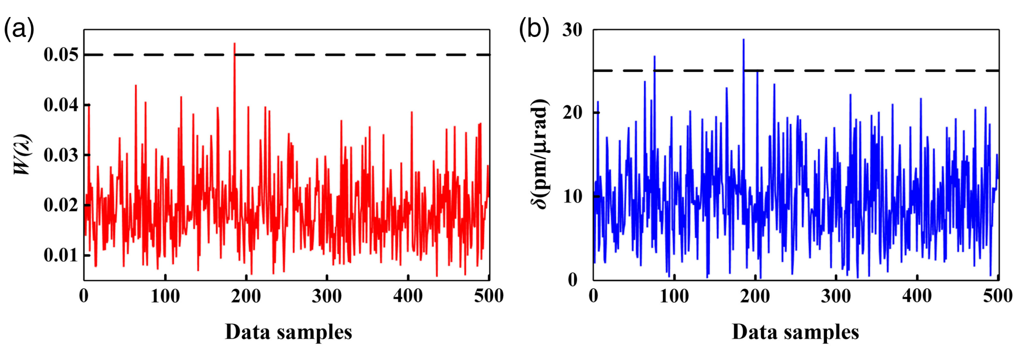

Fig. 7 Tolerance analysis results of the (a) wavefront error and (b) coupling coefficient.

6 Conclusion

The optical system of the Taiji telescope has a particular design. The wavefront error not only should meet the requirements of the diffraction limit but also suppress the coefficient of TTL noise coupling to $\pm 25\ \text{pm}/\mu\text{rad}$. In this study, we designed a high-performance telescope with low wavefront error and coupling coefficient for the Taiji Program of space GW detection. In the design process, we established the initial structure based on the aberration theory and according to the design indicators and requirements of the telescope in the Taiji project. Furthermore, we optimized the initial structure using the established optimization method and design process. Finally, we completed the design of a 400-mm-aperture space GW telescope. In addition, we analyzed the wavefront error, coupling coefficient, and tolerance of the design results. The analysis results revealed that the proposed design has good performance. The RMS value of the full-field wavefront error is better than $0.005\,\lambda$ and the coupling coefficient is not more than $1.7\ \text{pm}/\mu\text{rad}$, thereby satisfying the requirements of the Taiji telescope. From the tolerance analysis, the wavefront error with 99.8% cumulative probability is $<0.05\,\lambda$. The coupling coefficient with 99.4% cumulative probability is within $\pm 25\ \text{pm}/\mu\text{rad}$, thereby satisfying the requirements of space GW detection.

Code, Data, and Materials Availability

With regard to the research results reported in the manuscript, this section declares that the codes, data, and materials used are available.

Acknowledgments

We thank our project partners for their assistance and valuable discussions. Miao Yu and Jiancong Li contributed equally to this work. This research was funded by the National Natural Science Foundation of China (Grant No. 62075214), the Science and Technology Plan Project of Guangdong Province (Grant No. X190311UZ190), and the Research and Development Projects in Key Areas of Guangdong Province (Grant No. 2020B1111040001). The authors declare that they have no known competing financial interests or personal relationships that could have appeared to influence the work reported in this paper.

References

1. J. C. Livas et al., "Optical telescope system-level design considerations for a space-based gravitational wave mission," *Proc. SPIE* **9904**, 99041K (2016).
2. K. Danzmann. "LISA: laser interferometer space antenna for gravitational wave measurements," *Class. Quantum Grav.* **13**(11), A247 (1996).
3. Z. Luo et al., "The Taiji program: a concise overview," *Prog. Theor. Exp. Phys.* **2021**(05), A108 (2021).
4. Z. Luo et al., "A brief analysis to Taiji: science and technology," *Results Phys*, **16**, 102918 (2020).
5. J. Luo et al., "TianQin: a space-borne gravitational wave detector," *Class. Quantum Grav.* **33**(03), 035010 (2016).
6. S. R. Sankar et al., "Optical telescope design for a space-based gravitational-wave mission," *Proc. SPIE* **9143**, 914314 (2014).
7. D. Karsten et al., "LISA assessment study report (Yellow Book)," ESA/SRE, 2011, https://sci.esa.int/documents/35005/36499/1567258681608-LISA_YellowBook_ESA-SRE-2011-3_Feb2011.pdf.
8. Y. Zhao et al., "Tilt-to-length noise coupled by wave-front errors in the interfering beams for the space measurement of gravitational waves," *Opt. Express.* **28**(17), 25545–25561 (2020).
9. C. P. Sasso et al., "Coupling of wavefront errors and pointing jitter in the LISA interferometer: misalignments of the interfering wavefronts," *Class. Quantum Grav.* **35**(24), 5002 (2019).
10. S. R. Sankar et al., "Optical alignment and wavefront error demonstration of a prototype LISA telescope," *Class. Quantum Grav.* **37**(06), 065005 (2020).
11. M. Chwalla et al., "Design and construction of an optical test bed for LISA imaging systems and tilt-to-length coupling," *Class. Quantum Grav.* **33**(24), 245015 (2016).
12. S. Schuster et al., "Vanishing tilt-to-length coupling for a singular case in two-beam laser interferometers with Gaussian beams," *Appl. Opt.* **54**(5), 1010–1014 (2014).
13. A. J. Weaver et al., "Wavefront error based tilt-to-length noise analysis for the LISA transmitted beam," *Class. Quantum Grav.* **39**(19), 195016 (2022).
14. Y Zhao et al., "The far-field optical path noise coupled with the pointing jitter in the space measurement of gravitational waves," *Appl. Opt.* **60**(2), 438–444 (2021).

15. J. C. Livas et al., "Telescopes for space-based gravitational wave missions," *Opt. Eng.* **52**(9), 091811 (2013).
16. Z Fan et al., "High performance telescope system design for the TianQin project," *Class. Quantum Grav.* **39**(19), 195017 (2022).
17. D. Karsten et al., "LISA laser interferometer space antenna," ESA, 2017, https://www.elisascience.org/files/publications/LISA_L3_20170120.pdf.
18. J. Li et al., "Optical design of space gravitational wave detection telescope," *Chin. Opt.* **15**(4), 761–769 (In Chinese) (2022).
19. Z. Qin et al., "Desensitization design method for freeform TMA optical systems based on initial structure screening," *Photonics* **9**(8), 544 (2022).
20. X. Liu et al., "Design method of freeform off-axis multi-mirror optical systems," *Photonics* **9**(8), 534 (2022).
21. Y Zhao et al., "Method to remove tilt-to-length coupling caused by interference of flat-top beam and Gaussian beam," *Appl. Sci.* **9**, 4112 (2019).
22. J. Li, "Optical system design of large aperture space gravitational wave," Telescope.nb. figshare. Software (2022).
23. J. Li et al. "Evaluation method for the design results of space gravitational-wave telescopes," *Meas. Sci. Technol.* **34**, 055409 (2023).

Miao Yu received his bachelor's degree from Foshan University of Science and Technology in 2022. He is currently a graduate student at Foshan University of Science and Technology. His current research interest is in optical systems of space gravitational wave telescopes.

Jiancong Li received his bachelor's degree from Foshan University of Science and Technology in 2020. He is currently a postgraduate student at Foshan University of Science and Technology. At present, he is mainly engaged in the research of optical system design.

Yanxiong Wu received the PhD from the Changchun Institute of Optics, Fine Mechanics and Physics, Chinese Academy of Sciences, Changchun, China, in 2015. He is currently a professor with the School of Physics and Optoelectronic Engineering, Foshan University, Foshan, China. His research interests include optical instrument design, optical system design, and computational optical imaging.

Biographies of the other authors are not available.